Design and EM-driven Optimization Of A Compact Low Profile Circularly Polarized Wide-slot CPW-fed Antenna For Broadband Applications

Ubaid Ullah and Slawomir Koziel
Engineering Optimization & Modelling Centre
Reykjavik University, 101 Reykjavik, Iceland
ubaidu@ru.is, koziel@ru.is

***Abstract*—The paper presents design and optimization procedure of a compact circularly-polarized antenna for broadband applications. The major design challenge is a large number of geometry parameters (>20) which have to be simultaneously adjusted in order to achieve the best possible antenna performance. At the same time, several performance figures have to be handled, including bandwidth, reflection characteristic, and axial ratio (AR). As straightforward optimization involving all parameters and specifications fails in this case, a multi-stage optimization procedure is implemented that switches between design objectives and gradually increases the number of geometry parameters to be tuned. As a result, a compact structure of only 25 mm × 25 mm is achieved featuring –10 dB bandwidth of 44% and 3dB AR bandwidth of 35%. The structure is favorably compared to competitive designs reported in the literature.**

Keywords—Circularly polarized antennas; compact antennas; microstrip antennas; EM-driven design; design optimization.

I. INTRODUCTION

Continuous and rapid development of modern wireless communication systems, in particular miniaturization trends, create demand for compact-size components. An antenna, being a vital part of any wireless communicating device, needs special attention as size reduction should be achieved without compromising its electrical and field performance. A particular class of antenna structures that are proving themselves to be of considerable importance are circularly polarized (CP) antennas. This is due to their excellent features such as extenuating multipath losses and interference, polarization mismatch, and reducing Faradays rotation effects [1], [2]. Traditionally used planar antennas are of microstrip patch type which suffers from inherited narrowband operation both in terms of both the impedance bandwidth and the axial ratio bandwidth (ARBW) [3]. This is a serious limitation as, nowadays, almost every communication system offers multi-functionality and to be able to achieve it, broadband operation of the antenna is imperative. Researchers have explored wide slot antennas which have shown a promising response in terms of the impedance bandwidth as well as AR bandwidth [4-5].

There are several types of antennas that have the ability to operate in a broadband manner, such as monopoles [6], dipoles [7], substrate integrated waveguide slot antennas [8], as well as the loop antennas [9]. One of many challenges that are associated with these type of structures is the necessity of implementing a complex feeding network that ensures excitation of orthogonal electric (E) and magnetic (H) field components required for circular polarization. On the other hand, employing coplanar waveguide (CPW) feeding techniques with symmetrical and asymmetrical configuration offers advantages of wideband operation, simple geometry configuration, ease of fabrication and integration with microwave integrated circuits [10]. With these advantages, CPW fed antennas mitigate the need of complex circuitry and offer more flexibility to the antenna designers.

An improvement of antenna performance (both in terms of electrical and field characteristics but also size reduction) can be obtained by introducing various topological modifications. However, these normally lead to increasing the structure complexity and the number of geometry parameters that have to be tuned. Practical design of complex structures requires rigorous numerical optimization of all antenna parameters and, for reliability purposes, has to be executed at the level of full-wave EM simulation models. This can be realized using conventional gradient-based algorithms [11], or, for improved computational efficiency, using surrogate-assisted techniques [12].

In this paper, a modified E-shape wide slot CP antenna excited by an asymmetrical CPW stripline feed is proposed along with its design optimization procedure. The orthogonal modes were launched the antenna by placing a parasitic half rectangular loop next to the stripline extended from the asymmetric ground plane. Due to a large number of geometry parameters and several figures of interest considered, an iterative optimization procedure has been developed that alternates between various design objectives and increased the number of parameters considered as a given stage of the design process. The main optimization engine is a trust-region

978-1-5386-5204-6/18/$31.00@2018 IEEE

Authorized licensed use limited to: INDIAN INSTITUTE OF TECHNOLOGY KANPUR. Downloaded on March 23,2024 at 06:23:33 UTC from IEEE Xplore. Restrictions apply.
978-1-5386-5204-6/18/$31.00 ©2018 IEEE

gradient search algorithm. The final design features a compact in size (25 mm × 25 mm footprint) and broadband CP characteristics with a 10 dB return loss bandwidth of 45% and 3 dB AR bandwidth of 35%.

II. Antenna Geometry and Design Optimization Methodology

This section outlines the proposed antenna geometry as well as the optimization strategy developed to handle its large number of adjustable parameters and design specifications imposed on the structure.

A. Antenna Design

The main idea of the proposed design was inspired by the conventional wide square slot antenna which is well known for wideband operation both in linear and circular polarization. The proposed broadband wide-slot antenna was designed on a laminated rogers substrate RO4003C with permittivity of 3.38, tangent loss 0.0027, and thickness of 0.813 mm. Numerical simulation and EM driven optimization were carried out in the time domain using CST Microwave Studio. The computational model of the antenna is equipped with the SMA connector.

The antenna is fed by a CPW with the asymmetrical ground plane at the top and the modified E-shape slot on the bottom ground plane. The width of the strip line (Wm) and the gape (g) between the ground plane and the feed line is fixed at 50 Ω for a single port excitation. The parameterized front and back view of the proposed antenna is shown in Fig. 1(a) and 1(b), respectively. The antenna geometry is described by 22 adjustable parameters denoted as $\boldsymbol{x} = [L_1\ L_2\ L_3\ L_4\ W_1\ W_2\ W_3\ W_4\ L_{g2}\ L_c\ W_c\ L_{c1}\ W_{c1}\ L_{c2}\ W_{c2}\ L_{c3}\ W_{c3}\ L_{c4}\ W_{c4}\ d_1\ d_2\ d_3]^T$. Other parameters are fixed: W_m=1.55*,* g = 0.6075 (to ensure 50 ohm input impedance), L_m = 15.5 (fixed at $\lambda/4$ of the center frequency with respect to the impedance bandwidth), L_5 = 3.12, W_5 = 0.94, W_{g1} = 10.12*,* L_{g1} = 5, W_{g2} = 12.12, d_4 = 1.56 (values set based on the initial experiments and fixed due to low sensitivity), L_s = 25, W_s = 25, L_g = 25, W_g = 23 (due to fixed antenna size assumed). The unit for all dimensions is mm.

The broadband CP operation is mainly attributed to the modified wide E-slot and the asymmetric feeding geometry of the strip line and the half rectangular ring coupled capacitively to the main feed line. The orthogonal modes necessary for CP were adjusted using an offset value of d_1, d_2 and d_3.

B. Design Problem and Optimization Algorithm

The antenna is supposed to operate within the frequency range of 4.0 GHz to 5.65 GHz, which covers several practically utilized bands such as WLAN (4.9, 5, 5.2 GHz), WiMax (5.5 GHz), or INSAT (receive frequency) 4.2-4.8 GHz. Let us denote by $BW_S(\boldsymbol{x})$ the antenna impedance bandwidth (i.e., the continuous frequency range for which $|S_{11}| \leq -10$ dB), by $S(\boldsymbol{x})$ the maximum reflection level within the 4.0 GHz to 5.65 GHz frequency range, and by $AR(\boldsymbol{x})$ the maximum value of the axial ratio (AR) within the same range. An explicit dependence on adjustable parameter vector $\boldsymbol{x}$ is indicated to facilitate further description.

The design specifications are as follows:

- Ensure that $S(\boldsymbol{x}) \leq -10$ dB;
- Maximize $BW_S(\boldsymbol{x})$ around 5 GHz;
- Minimize $AR(\boldsymbol{x})$;

The primary design challenges include: (i) high cost of EM simulation of the antenna structure, (ii) a large number of geometry parameters, and (iii) necessity of simultaneous handling of several performance figures. Straightforward optimization of all parameters with respect to all specifications fails. Instead, an multi-stage procedure is utilized as described below. The generic optimization task is formulated as follows:

$$\boldsymbol{x}^* = \arg\min_{\boldsymbol{x}} U\left(BW_S(\boldsymbol{x}), S(\boldsymbol{x}), AR(\boldsymbol{x})\right) \tag{1}$$

where U is the objective function. We consider two separate sub-problems. The first one is to optimize the antenna impedance bandwidth with the objective function defined as

$$U_S\left(BW_S(\boldsymbol{x}), S(\boldsymbol{x}), AR(\boldsymbol{x})\right) = -BW_s(\boldsymbol{x}) + \beta_S c_S(S(\boldsymbol{x}))^2 \tag{2}$$

where $c_S(S(\boldsymbol{x})) = \max\{(S(\boldsymbol{x}) + 10, 0\}/10$ is a penalty function that "measures" a relative violation of the condition $S(\boldsymbol{x}) \leq -10$ dB, and β_S is a penalty factor.

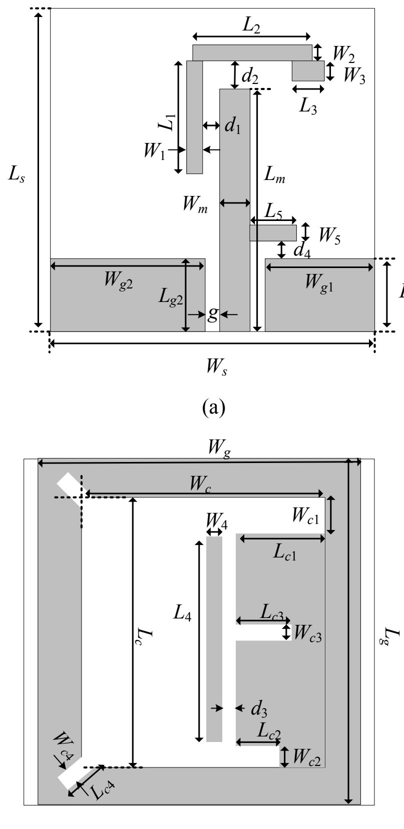

Fig. 1. Geometry of the proposed CP antenna: (a) front view (b) back view.

978-1-5386-5204-6/18/$31.00@2018 IEEE

Authorized licensed use limited to: INDIAN INSTITUTE OF TECHNOLOGY KANPUR. Downloaded on March 23,2024 at 06:23:33 UTC from IEEE Xplore. Restrictions apply.

The purpose of solving (1) with the objective function (2) is to increase the antenna bandwidth and to ensure sufficient matching within the 4.0 GHz to 5.65 GHz range.

The objective function for the second sub-problem is defined as

$$U_{AR}\left(BW_S(\boldsymbol{x}), S(\boldsymbol{x}), AR(\boldsymbol{x})\right) = AR(\boldsymbol{x}) + \beta_S c_S (S'(\boldsymbol{x}))^2 \tag{3}$$

Here, the goal is to minimize the maximum in-band axial ratio. The symbol $S'(\boldsymbol{x})$ denotes the maximum reflection level within the bandwidth obtained upon solving (1) with the objective function (2).

Also, in order to facilitate the optimization process, at the initial stage, only 12 geometry parameters are utilized denoted as $\boldsymbol{x}_0 = [L_1\ W_1\ L_2\ W_2\ L_3\ W_3\ L_4\ W_4\ L_{g2}\ d_1\ d_2\ d_3]^T$. These parameters were selected through sensitivity analysis (i.e., those with respect to which both design goals are the most sensitive). The remaining variables are included in the second design stage.

The overall flow of the optimization process is the following:

1. Solve the problem (1) with the objective function (2) for a reduced parameter set $\boldsymbol{x}_0$:
$$\boldsymbol{x}_0^* = \arg\min_{\boldsymbol{x}} U_S\left(BW_S(\boldsymbol{x}_0), S(\boldsymbol{x}_0), AR(\boldsymbol{x}_0)\right)$$
2. Starting from $\boldsymbol{x}_0^*$, solve the problem (1) with the objective function (3) for a reduced parameter set:
$$\boldsymbol{x}_0^{**} = \arg\min_{\boldsymbol{x}} U_{AR}\left(BW_S(\boldsymbol{x}_0), S(\boldsymbol{x}_0), AR(\boldsymbol{x}_0)\right)$$
3. Solve the problem (1) with the objective function (2) for the entire parameter set (the components of $\boldsymbol{x}_0^{**}$ are used as initial values):
$$\boldsymbol{x}^* = \arg\min_{\boldsymbol{x}} U_S\left(BW_S(\boldsymbol{x}), S(\boldsymbol{x}), AR(\boldsymbol{x})\right)$$
4. Identify the final design by solving (1) with the objective function (3) for the entire parameter set, starting from $\boldsymbol{x}^*$:
$$\boldsymbol{x}^{**} = \arg\min_{\boldsymbol{x}} U_{AR}\left(BW_S(\boldsymbol{x}), S(\boldsymbol{x}), AR(\boldsymbol{x})\right)$$

All sub-problems are solved using a trust-region gradient search [18] with the antenna response gradients estimated using finite differentiation. Sequential optimization (first for impedance bandwidth enhancement, then for axial ratio improvement) allows for efficient handling of all performance figures. In particular, ensuring sufficient matching provides a feasible starting point for AR optimization.

III. Results and Discussion

The antenna of Fig. 1 has been optimized using the procedure described in Section II. The lower and upper bounds for geometry parameters during the first two stages are $\boldsymbol{l}_0 = [7\ 9\ 2\ 2\ 0.5\ 0.5\ 1.5\ 0.5\ 4\ -1\ -1\ -1]^T$ and $\boldsymbol{u}_0 = [9\ 11\ 4\ 4\ 1.5\ 1.5\ 2.5\ 1.5\ 6\ 1\ 1\ 1\ ]^T$. The initial design was $\boldsymbol{x}_0^{init} = [8\ 10\ 3\ 3\ 1.2\ 1.0\ 2.2\ 0.8\ 5.0\ 0.0\ 0.0\ 0.0]^T$. The optimized design is $\boldsymbol{x}_0^{**} = [7.56\ 9.78\ 2.18\ 3.13\ 1.24\ 1.42\ 1.95\ 0.94\ 5.11\ -0.071\ -0.034\ 0.22]^T$.

In the next stage of the optimization process, the initial design was $\boldsymbol{x}^{init} = [7.56\ 9.78\ 2.18\ 3.13\ 1.24\ 1.42\ 1.95\ 0.94\ 5.11\ 17.88\ 16.4\ 5\ 2.5\ 3\ 1.82\ 2.5\ 1\ 3\ 1.4\ -0.071\ -0.034\ 0.022]^T$, and the bounds $\boldsymbol{l} = [7\ 8.5\ 1.5\ 2.5\ 0.5\ 1\ 1.5\ 0.5\ 4.5\ 16\ 15\ 4\ 2\ 2\ 1\ 2\ 0.5\ 2.5\ 0.5\ -1\ -1\ -1]^T$, and $\boldsymbol{u} = [8\ 10\ 2.5\ 3.5\ 1.5\ 2\ 2.5\ 1.5\ 5.5\ 18\ 17\ 6\ 3\ 2.5\ 2\ 3\ 1.5\ 3.5\ 1.5\ 1\ 1\ 1]^T$. The final optimized values are listed in Table I.

Figure 2 shows the antenna reflection response at the initial design as well as at $\boldsymbol{x}_0^{**}$ and the final design $\boldsymbol{x}^{**}$. A broad impedance bandwidth of 44% (3.9 GHz to 6.2 GHz) has been achieved with the impedance matching value reaching beyond –35dB which assures maximum energy transfer from the input port to the resonator. Furthermore, the axial ratio bandwidth (ARBW) of the final design is as wide as 34%.

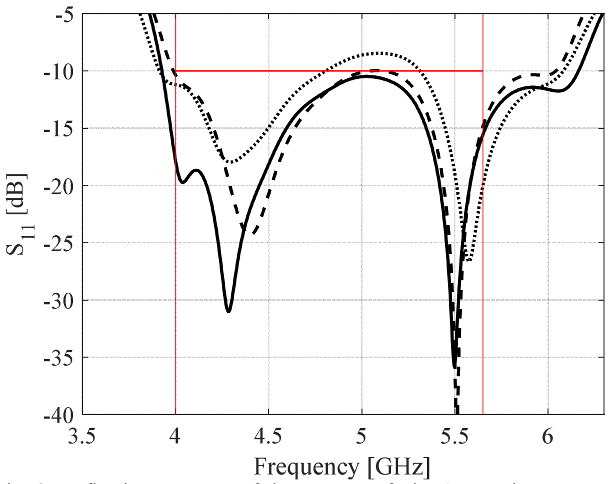

Fig. 2: Reflection response of the antenna of Fig. 1 at various stages of the design process: initial design (····), optimization with reduced parameter set $\boldsymbol{x}_0^{**}$ (- - -), final design $\boldsymbol{x}^{**}$ (—). Bandwidth of interest and –10 dB level marked with vertical and horizontal lines, respectively.

TABLE I Optimized Antenna Geometry Parameters

Parameter	L_s	W_s	L_g	W_g	L_{g1}	W_{g1}
Value (mm)	25	25	25	23	5	10.12
Parameter	L_{g2}	W_{g2}	L_m	W_m	L_1	W_1
Value (mm)	5.11	12.12	15.5	1.55	7.55	1.3
Parameter	L_2	W_2	L_3	W_3	L_4	W_4
Value (mm)	8.7	1.7	2.18	1.95	3.12	0.94
Parameter	L_c	W_c	L_{c1}	W_{c1}	L_{c2}	W_{c2}
Value (mm)	17.96	16.4	5.13	2.63	2.87	1.69
Parameter	L_{c3}	W_{c3}	L_{c4}	W_{c4}	g	d_1
Value (mm)	2.37	0.91	3.12	1.37	0.6075	1.656
Parameter	d_2	d_3	d_4	L_5	W_5	
Value (mm)	1.03	0.57	1.56	3.12	0.94	

978-1-5386-5204-6/18/$31.00@2018 IEEE

Authorized licensed use limited to: INDIAN INSTITUTE OF TECHNOLOGY KANPUR. Downloaded on March 23,2024 at 06:23:33 UTC from IEEE Xplore. Restrictions apply.

The proposed antenna has been compared in terms of ARBW, impedance bandwidth, and footprint with recent state-of-the-art CP antennas from the literature. The structures operating within similar frequency ranges have been selected for a comparison. As other structures are designed on substrates with different dielectric characteristics, for the sake of fair comparison, the dimensions have been recalculated in terms of the guided wavelength (λ_g). It can be observed from Table II that the proposed antenna exhibits better performance with respect to all major performance figures, including impedance bandwidth, ARBW, and the size.

IV. Conclusion

In this work, a novel structure of a compact low profile circular polarization antenna has been presented along with rigorous design optimization of its geometry parameters. For feasibility reasons, the optimization process is decomposed into two stages (impedance bandwidth enhancement and axial ratio improvement) and two cycles, first with a reduced parameter set and the second with a full parameter set. The final design features a small size and is favorably compares to state-of-the-art CP antennas reported in the literature with respect to both electrical and field properties.

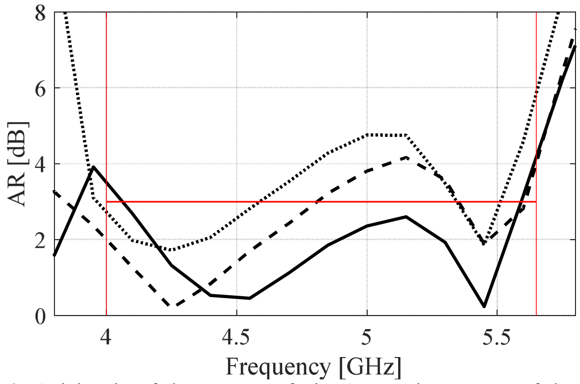

Fig. 3: Axial ratio of the antenna of Fig. 1 at various stages of the design process: initial design (····), optimization with reduced parameter set $\boldsymbol{x}_0^{**}$ (- - -), final design $\boldsymbol{x}^{**}$ (—).Bandwidth of interest and 3 dB level marked with vertical and horizontal lines, respectively.

TABLE II Comparison with State-of-the-Art CP Antennas

Ref.	% AR$	% IBW*	Antenna footprint (mm²)	λ_g^2	Year
[13]	27	111	2500	1.58	2013
[14]	15.4	----	900	0.95	2010
[15]	26.9	27	2500	1.58	2017
[16]	22	37	2500	2.00	2015
[17]	14	27	400	0.63	2015
This work	35	44	625	0.71	2018

$ % AR stands for fractional axial ratio bandwidth.
* % IBW stands for fractional impedance bandwidth.

Acknowledgement

The authors would like to thank Dassault Systemes, France, for making CST Microwave Studio available. This work was supported in part by the Icelandic Centre for Research (RANNIS) Grant 174114051.

References

[1] F. Khosravi and P. Mousavi, “Bidirectional same-sense circularly polarized slot antenna using polarization converting surface,” *IEEE Antenna Wireless Propag. Lett.*, vol. 13, no. 1, pp. 1652–1655, 2014.

[2] K. Agarwal, Nasimuddin, and A. Alphones, “RIS-based compact circularly polarized microstrip antennas,” *IEEE Trans. Antenna Prop.*, vol. 61, no. 2, pp. 547–555, Feb. 2013.

[3] H. Bagheroghli, “A novel circularly polarized microstrip antenna with two connected quasi monopoles for wideband applications,” *IEEE Antennas Wireless Propag. Lett*., vol. 12, no.1, pp. 1343–1346, 2013.

[4] J. S. Row, “The design of a squarer-ring slot antenna for circular polarization,” *IEEE Trans. Antennas Propag*., vol. 53, no. 6, pp. 1967–1972, Jun. 2005.

[5] P. N. Rao and N. V. S. N. Sarma, “Fractal boundary circularly polarized single feed microstrip antenna,” *Electron. Lett.,* vol. 44, pp. 713–714, Jun. 2008.

[6] K. M. Mak and K. Luk, “A circularly polarized antenna with wide axial ratio beamwidth,” *IEEE Trans. Antennas Propag*., vol. 57, no. 10, pp. 3309–3312, Oct. 2009.

[7] R. Pazoki, A. Kiaee, P. Naseri, H. Moghadas, H. Oraizi and P. Mousavi, “Circularly polarized monopole L-shaped slot antenna with enhanced axial-ratio bandwidth,” *IEEE Antenna Wireless Propag. Lett.*, vol. 15, pp. 1073-1076, 2016.

[8] Y. Li, Z. Chen, X. Qing, Z. Zhnag, J. Xu, and Z. Feng, “Axial ratio bandwidth enhancement of 60-GHz substrate integrated waveguidefed circularly polarized LTCC antenna array,” *IEEE Trans. Antennas Propag*., vol. 60, no. 10, pp. 4619–4636, Oct.2012.

[9] Y. Li, Z. Zhnag, and Z. Feng, “A sequential-phase feed using a circularly polarized shorted loop structure,” *IEEE Trans. Antennas Propag*., vol. 61, no. 3, pp. 1443–1447, Mar. 2013.

[10] M. A. Malek, S. Hakimi, S. K. Abdul Rahim and A. K. Evizal, "Dual-band CPW-fed transparent antenna for active RFID tags," in *IEEE Antennas and Wireless Propag. Lett.*, vol. 14, no 1, pp. 919-922, 2015.

[11] S. Koziel and S. Ogurtsov, “Model management for cost-efficient surrogate-based optimisation of antennas using variable-fidelity electromagnetic simulations,” *IET Microw, Antennas Propag*., vol. 6, no. 15, pp. 1643–1650, 2012.

[12] A. Bekasiewicz, and S. Koziel, “Structure and computationally-efficient simulation-driven design of compact UWB monopole antenna,” *IEEE Antenna Wireless Prop. Lett*., vol. 14, no1, pp. 1282−1285, 2015

[13] J. Y. Jan, C. Y. Pan, K. Y. Chiu and H. M. Chen, "Broadband CPW-fed circularly-polarized slot antenna with an open slot," in *IEEE Trans. on Antennas and Propa.* vol. 61, no. 3, pp. 1418-1422, March 2013.

[14] G. Beigmohammadi, C. Ghobadi, J. Nourinia and M. Ojaroudi, “Small square slot antenna with circular polarisation characteristics for WLAN/WiMAX applications,” *Electron. Lett.*, vol. 46, no. 10, pp. 672-673, 2010

[15] R. Chowdhury, R. Kumar, and R. K. Chaudhary, “A coaxial probe fed wideband circularly polarized antenna using unequal and adjacent-slided rectangular dielectric resonators for WLAN applications,” *Int J. RF Microw. Comput. Aided Eng*., pp. 1–9, 2017.

[16] S. Fakhte, H. Oraizi, R. Karimian and R. Fakhte, "A new wideband circularly polarized stair-shaped dielectric resonator antenna," in *IEEE Trans. Antennas and Propag.,* vol. 63, no. 4, pp. 1828-1832, April 2015.

[17] Y. Ojaroudi, N. Ojaroudi, and N. Ghadimi, “Circularly polarized microstrip slot antenna with a pair of spur-shaped slits for WLAN applications,” *Microw. Opt. Technol. Lett*., vol. 57, pp. 756–759, 2015

[18] S. Koziel, J.W. Bandler, and Q.S. Cheng, “Robust trust-region space-mapping algorithms for microwave design optimization,” *IEEE Trans. Microwave Theory and Tech.*, vol. 58, no. 8, pp. 2166-2174, 2010.

Authorized licensed use limited to: INDIAN INSTITUTE OF TECHNOLOGY KANPUR. Downloaded on March 23,2024 at 06:23:33 UTC from IEEE Xplore. Restrictions apply.